

Fabrication of Ti–Al–Zr alloy oxide nanotube arrays in organic electrolytes by anodization

Rongqing Xu · Jianling Zhao · Jinliang Tao ·
Xixin Wang · Yangxian Li

Received: 22 November 2007 / Revised: 20 February 2008 / Accepted: 29 February 2008 / Published online: 18 March 2008
© Springer Science+Business Media B.V. 2008

Abstract We report the formation of self-organized Ti–Al–Zr alloy oxide nanotube arrays at different fluoride concentrations in formamide and glycerol electrolytes. The nanotube morphology is strongly influenced by the fluoride concentration, applied potential and reaction time. Titanium alloy (Ti–Al–Zr) oxide nanotube arrays with a length of about 6.13 μm , a pore diameter of 116 nm and wall thickness of 55 nm were prepared at 50 V for 24 h in formamide and glycerol mixtures (volume ratio 1:1) with addition of 1.0 wt% NH_4F . The as-prepared nanotubes were amorphous and alloy oxide crystals appeared after annealing in air at 400 and 600 $^\circ\text{C}$ for 3 h.

Keywords Titanium alloy oxide · Nanotube · Anodization

1 Introduction

Fabrication of oxide nanotube arrays on Ti by electrochemical methods has attracted much attention and various applications including dye-sensitizing [1, 2], wettability [3], photocatalysis [4–7], bone growth and regeneration [8–12], environmental applications [13], solar cells [14] and catalysis [15–17] have been explored with considerable success. Electrochemical formation of nanotubes on titanium alloys such as Ti–Al, Ti–Zr and Ti–Mn has recently been studied [18–23]. Zirconia and alumina are widely used catalyst

carriers [24–26] and it is reasonable to presume that doping of zirconia and alumina into the titania nanotube may improve their catalytic properties. However, to the best of our knowledge, no study on the formation of nanotubes on Ti–Al–Zr alloys has been done. In the present work, we explore the formation of self organized Ti–Al–Zr alloy oxide nanotube arrays by anodic oxidation in formamide and glycerol electrolytes. Effects of the kind of electrolyzer, the concentration of F^- and time on the microstructure of the nanotubes have been studied. Crystal transformation of the as-prepared samples at higher temperature has also been confirmed.

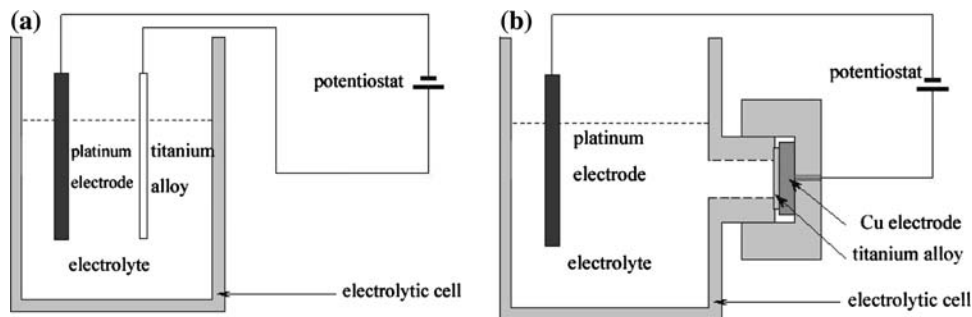
2 Experimental

Ti–Al–Zr alloy foils (Al-5.53%, Zr-4.35%), with a thickness of 0.15 mm, were prepared by Ar-arc melting. Ti, Al and Zr samples were commercial foils with a purity of 99.9%, 99.99% and 99.7% respectively. The samples were sonicated in ethanol and deionized water before anodization. Anodization experiments were conducted in a two-electrode system at constant potential. Two kinds of electrolyzer were used. In electrolyzer-1 (Fig. 1a) the sample was immersed in the solution directly. In electrolyzer-2 (Fig. 1b) the sample was pressed against an O-ring in the electrochemical cell leaving 1 cm^2 of the sample surface exposed to the electrolyte. Ti–Al–Zr alloy foils ($8 \times 5 \times 0.15 \text{ mm}^3$) were used as anode while platinum ($30 \times 20 \times 0.1 \text{ mm}^3$) was used as cathode. Electrolytes were formamide (FA) and glycerol (volume ratio 1:1) with addition of (0.5–2.0 wt%) NH_4F . All electrolytes were prepared from analytical grade chemicals and deionized water. All experiments were done at room temperature. During the experiments the solutions were stirred using a magnetic stirrer. After anodization the

R. Xu · J. Zhao (✉) · J. Tao · X. Wang · Y. Li (✉)
School of Material Science and Engineering, Hebei University
of Technology, Tianjin 300130, China
e-mail: hebutzhaoj@126.com

Y. Li
e-mail: yxli@jsmail.hebut.edu.cn

Fig. 1 The schematic diagram of the experiment set (a) electrolyzer-1, (b) electrolyzer-2



samples were rinsed with deionized water. In order to study the crystal phase transition, the nanotube samples were annealed at different temperatures from 200 to 600 °C in air for 3 h with heating and cooling rates of 10 °C min⁻¹.

The microstructures of the nanotubes were characterized using a scanning electron microscope (SEM, PhilipsXL30) operating at an accelerating voltage of 25 kV. The crystal structure of the oxide was characterized by X-ray diffraction (XRD, Phillips X'pert MPD PW3040). Direct SEM cross-sectional observations were carried out on mechanically bent samples.

3 Results and discussion

Figure 2 shows SEM images of the structures after anodization at 50 V in FA + glycerol + 0.5 wt% NH₄F solution for 24 h in both kinds of electrolyzer. The microstructure of the nanotubes prepared in electrolyzer-1 is better than that prepared in electrolyzer-2. The pore diameter of the nanotubes in electrolyzer-1 is approximately 107 nm, while the wall thickness is 25 nm (Fig. 2a). The pore diameter of the nanotubes in electrolyzer-2 is approximately 81 nm and the wall thickness is 50 nm (Fig. 2b).

Clearly, the pore diameter of the former is bigger than that of the latter, but the wall thickness of the former is thinner. This might be due to the bigger resistance of transfer in electrolyzer-2 than that in electrolyzer-1. Obviously there is a long and narrow groove in front of the

anode in electrolyzer-2, which is not beneficial to mass transfer. The high viscosity of the organic electrolyte has a strong influence on mass transfer [27].

We investigated the processing parameters affecting the formation of oxide nanotube arrays with a series of comparative experiments in electrolyzer-1. Figure 3 shows the SEM images of titanium alloy oxide nanotube arrays formed in FA + glycerol + 1.0 wt% NH₄F at 50 V for different times. Figure 3a, b shows SEM images of nanotubes formed for 24 h. The nanotubes show a distinct smooth and straight morphology with a length of about 6.13 μm and an inner pore diameter of 116 nm with a wall thickness of 55 nm. Figure 3c shows a SEM image of the top-view formed for 48 h. It is clear from Fig. 3c that the nanotubes are open, with pore diameter of 106 nm and wall thickness of 61 nm. From Fig. 3d it is evident that the porous structure is open on the top and closed at the bottom of the layer for 72 h anodization. The resulting pore diameter was 110 nm and the wall thickness was 64 nm. From 24 to 72 h, the inner diameter and the wall thickness had no obvious difference, but the amount of precipitate covering the surface was reduced. The sample oxidized for 24 h (Fig. 3a) shows part of the surface covered with oxide nanotubes. The sample oxidized for 48 h (Fig. 3c) shows a large area covered with the porous structure. After 72 h (Fig. 3d) well structured areas of pores cover almost the entire surface. The amount of precipitate on the top of the porous structure is negligible. In addition, experiment results indicate that the nanotube length did not increase with anodization time after 24 h; the morphology of the

Fig. 2 The SEM images of the nanotubes surface for Ti–Al–Zr alloy anodization at 50 V in FA + glycerol + 0.5 wt% NH₄F solution for 24 h with two kinds of electrolyzer. (a) In electrolyzer-1, (b) in electrolyzer-2

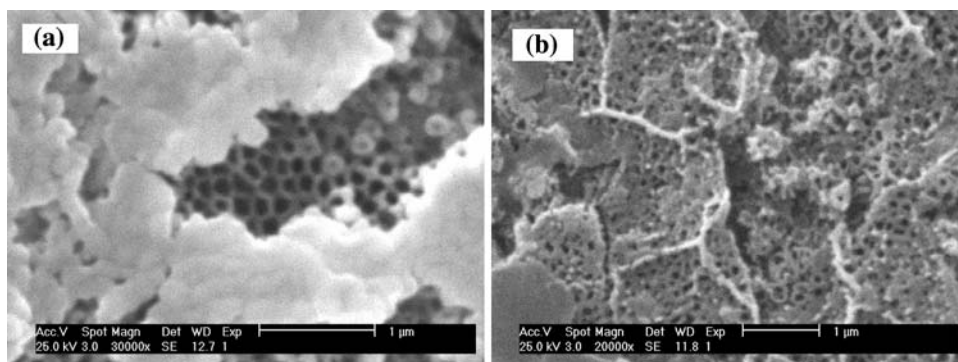


Fig. 3 SEM images of oxide nanotube layers formed in FA + glycerol + 1.0 wt% NH_4F at 50 V: (a, b) 24 h, top-view and the cross-sectional view; (c) 48 h, top-view; (d) 72 h, top-view, in the insets the bottom view of the nanotubes are shown

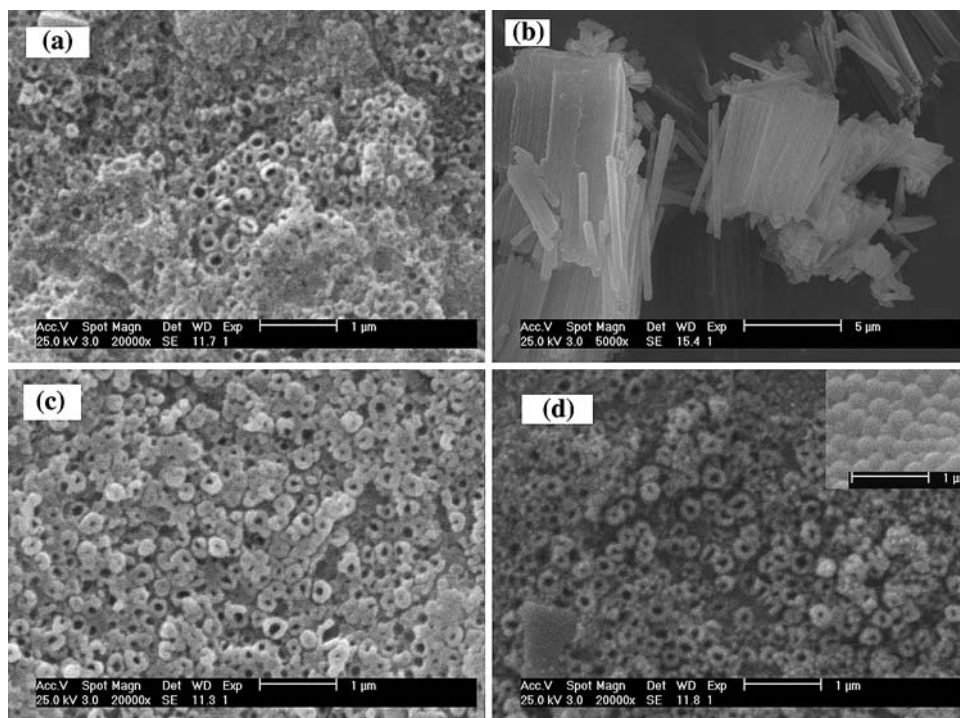
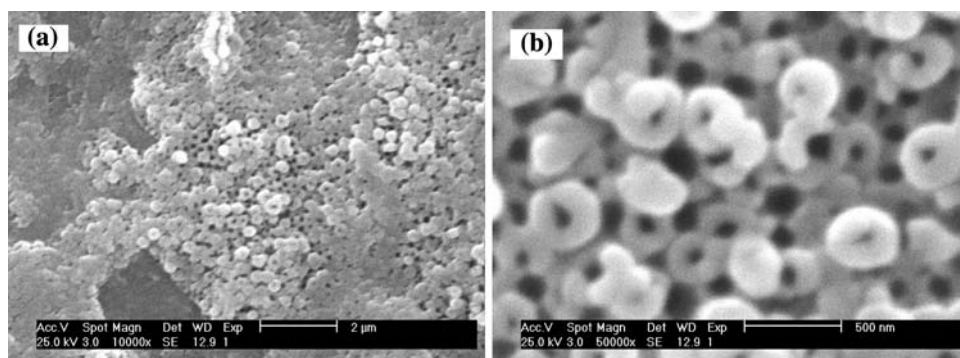


Fig. 4 SEM images of oxide nanotube layers formed in FA + glycerol + 2.0 wt% NH_4F at 50 V for 24 h (a) top view, (b) the magnified views of the top



bottom of the nanotubes was similar for different anodization times.

Figure 4 shows the surface morphology of a sample anodized in formamide and glycerol mixtures containing 2.0 wt% NH_4F at 50 V for 24 h. Compared with Figs. 2a and 3a, the porous surface shows a uniform, regular structure with a pore diameter of approximately 115 nm. This suggests that the amount of NH_4F strongly influences the precipitates on the surface. This can be ascribed to dissolution of the electrochemically formed oxide as soluble fluoro-complexes $[\text{MF}_6]^{X-}$, which go into solution.

Oxide nanotube pore sizes are different under different anodization potentials. Figure 5 shows a SEM image of titanium alloy oxide nanotubes formed at 100 V for 24 h with addition of 1.0 wt% NH_4F . The surface is rough and few pores can be seen. The dissolution of oxide nanotubes

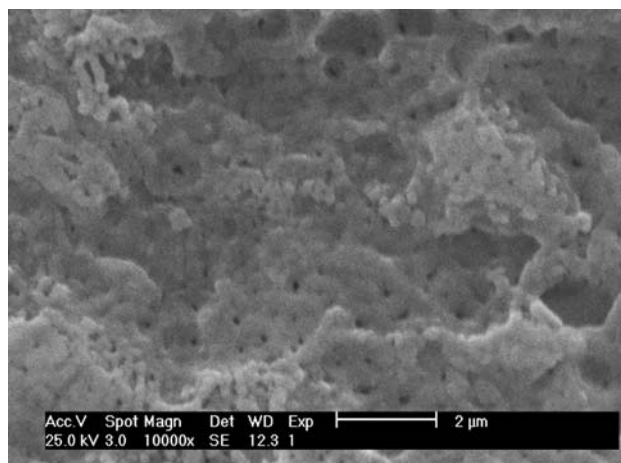


Fig. 5 SEM image of oxide nanotube layers formed in FA + glycerol + 1.0 wt% NH_4F at 100 V for 24 h

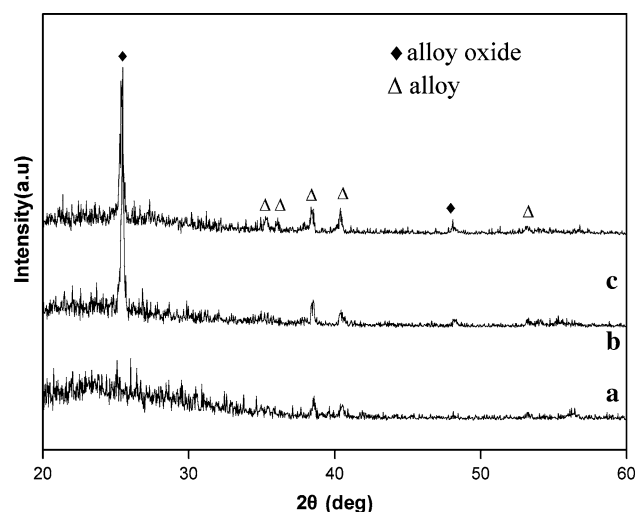
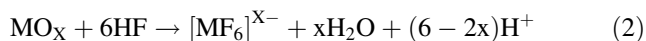
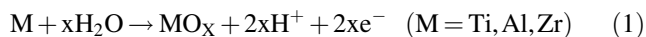


Fig. 6 The XRD patterns of oxide nanotube film formed after anodization in FA + glycerol + 1.0 wt% NH_4F at 50 V for 24 h and after annealing in air at (a) 200 °C, (b) 400 °C, (c) 600 °C for 3 h with heating and cooling rate $10\text{ }^\circ\text{C min}^{-1}$

results in their connection with each other because the potential impacts the electrochemical etching rate. As the potential increases, the electrochemical etching rate and current density also increase. These effects appear to cause the pore walls to collapse before the formation of channels that form separate pores.

From these experiments it is clear that the anodization time, applied potential and the concentration of F^- are important parameters for fabricating oxide nanotube arrays by anodization. The formation of oxide nanotube formation in F^- -containing electrolytes is the result of two competitive processes which can be described as follows:



XRD investigations showed that as-formed oxide nanotubes were of amorphous nature. The samples were annealed at higher temperature to investigate the crystal transformation. Figure 6 shows the XRD patterns of oxide nanotube films formed after anodization in FA + glycerol + 1.0 wt% NH_4F at 50 V for 24 h and annealed in air at 200, 400, 600 °C for 3 h with heating and cooling at $10\text{ }^\circ\text{C min}^{-1}$. X-ray diffraction patterns show that some Ti alloy-peaks from the Ti alloy substrate are observed at 200 °C. After annealing for 3 h at 400 and 600 °C an intense peak around $2\theta = 25$ and a small peak at $2\theta = 48$ emerge. These are believed to originate from the oxide of Ti–Al–Zr alloy.

4 Conclusion

A titanium alloy (Ti–Al–Zr) oxide nanotube array with a length of about 6.13 μm , a pore diameter of 116 nm and

wall thickness of 55 nm was prepared at 50 V for 24 h in formamide and glycerol mixtures (volume ratio 1:1) with addition of 1.0 wt% NH_4F by anodization. The anodization time, the applied potential, the concentration of F^- and the kind of electrolyzer had a clear influence on the process. XRD patterns showed that as-formed oxide layers were amorphous; the alloy oxide structures appeared after annealing in air at 400 and 600 °C for 3 h.

Acknowledgments This work was supported by Tianjin Natural Science Foundation (07JCYBJC03300) and Natural Science Foundation of Hebei Province of China (E2007000044).

References

- Macak JM, Tsuchiya H, Ghicov A et al (2005) *Electrochem Commun* 7:1133
- Mor GK, Varghese OK, Paulose M et al (2006) *Sol Energ Mater Sol Cells* 90:2011
- Balaur E, Macak JM, Taveira L et al (2005) *Electrochem Commun* 7:1066
- Zhao J, Wang X, Sun T et al (2007) *J Alloys Compd* 434–435:792
- Ruan C, Paulose M, Varghese OK et al (2006) *Sol Energ Mater Sol Cells* 90:1283
- Turkevych I, Pihosh Y, Goto M et al (2007) Photocatalytic properties of titanium dioxide sputtered on a nanostructured substrate. *Thin Solid Films* (in press). doi: 10.1016/j.tsf.2007.04.083
- Paulose M, Mor GK, Varghese OK et al (2006) *J Photochem Photobiol A* 178:8
- Kasuga T (2006) *Thin Solid Films* 496:141
- Oh S, Finones RR, Daraio C, Chen L et al (2005) *Biomaterials* 26:4938
- Tsuchiya H, Macak JM, Muller L et al (2006) *J Biomed Mater Res A* 77:534
- Xiao X, Tian T, Liu R et al (2007) *Mater Chem Phys* 106:27
- Oh S, Jin S (2006) *Mater Sci Eng C* 26:1301
- Zhou Q, Ding Y, Xiao J et al (2007) *J Chromatogr A* 1147:10
- Shankar K, Mor GK, Prakasam HE et al (2007) Highly-ordered TiO_2 nanotube arrays up to 220 μm in length: use in waterphotoelectrolysis and dye-sensitized solarcells. *Nanotechnology*. doi: 10.1088/0957-4484/18/6/065707
- Eder D, Motta MS, Kinloch IA et al (2007) *Physica E* 37:245
- Macak JM, Schmidt-Stein F, Schmuki P (2007) *Electrochem Commun* 9:1783
- Wang M, Guo D, Li H (2005) *J Solid State Chem* 178:1996
- Tsuchiya H, Berger S, Macak JM et al (2007) *Electrochem Commun* 9:2398
- Yasuda K, Schmuki P (2007) *Adv Mater* 19:1757
- Yasuda K, Schmuki P (2007) *Electrochem Commun* 9:615
- Mohapatra SK, Raja KS, Misra M et al (2007) *Electrochim Acta* 53:590
- Macak JM, Tsuchiya H, Taveira L et al (2005) *J Biomed Mater Res* 75A:928
- Ghicov A, Schmuki P (2006) *Angew Chem Int Ed* 45:6993
- Liu X, Lu G, Yan Z (2005) *Appl Catal A Gen* 279:241
- Yamamoto N, Sato S, Takahashi R et al (2006) *J Mol Catal A: Chem* 243:52
- Parizotto NV, Rocha KO, Damyanova S et al (2007) *Appl Catal A Gen* 330:12
- Macak JM, Schmuki P (2006) *Electrochim Acta* 52:1258